

See discussions, stats, and author profiles for this publication at: <https://www.researchgate.net/publication/236926217>

Influence of Chemical and Physical Properties of Activated Carbon Powders on Oxygen Reduction and Microbial Fuel Cell Performance

ARTICLE *in* ENVIRONMENTAL SCIENCE & TECHNOLOGY · MAY 2013

Impact Factor: 5.33 · DOI: 10.1021/es401722j · Source: PubMed

CITATIONS

39

READS

50

3 AUTHORS, INCLUDING:



Cesar Nieto-Delgado

Instituto Potosino de Investigación Científica ...

18 PUBLICATIONS 232 CITATIONS

SEE PROFILE



Bruce E Logan

Pennsylvania State University

458 PUBLICATIONS 33,277 CITATIONS

SEE PROFILE

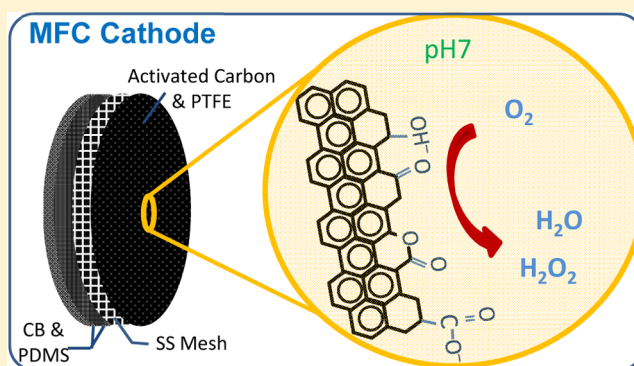
Influence of Chemical and Physical Properties of Activated Carbon Powders on Oxygen Reduction and Microbial Fuel Cell Performance

Valerie J. Watson, Cesar Nieto Delgado, and Bruce E. Logan*

Department of Civil and Environmental Engineering, The Pennsylvania State University, University Park, Pennsylvania 16802, United States

Supporting Information

ABSTRACT: Commercially available activated carbon (AC) powders made from different precursor materials (coal, peat, coconut shell, hardwood, and phenolic resin) were electrochemically evaluated as oxygen reduction catalysts and tested as cathode catalysts in microbial fuel cells (MFCs). AC powders were characterized in terms of surface chemistry and porosity, and their kinetic activities were compared to carbon black and platinum catalysts in rotating disk electrode (RDE) tests. Cathodes using the coal-derived AC had the highest power densities in MFCs ($1620 \pm 10 \text{ mW m}^{-2}$). Peat-based AC performed similarly in MFC tests ($1610 \pm 100 \text{ mW m}^{-2}$) and had the best catalyst performance, with an onset potential of $E_{\text{onset}} = 0.17 \text{ V}$, and $n = 3.6$ electrons used for oxygen reduction. Hardwood based AC had the highest number of acidic surface functional groups and the poorest performance in MFC and catalysis tests ($630 \pm 10 \text{ mW m}^{-2}$, $E_{\text{onset}} = -0.01 \text{ V}$, $n = 2.1$). There was an inverse relationship between onset potential and quantity of strong acid ($\text{p}K_{\text{a}} < 8$) functional groups, and a larger fraction of microporosity was negatively correlated with power production in MFCs. Surface area alone was a poor predictor of catalyst performance, and a high quantity of acidic surface functional groups was determined to be detrimental to oxygen reduction and cathode performance.



INTRODUCTION

Microbial fuel cells (MFCs) are a promising technology for treatment of wastewater streams in combination with electricity production.¹ MFCs reduce energy consumption for wastewater treatment through the elimination of the need for wastewater aeration and allow for the utilization of an untapped renewable energy source in the wastewater organic matter. MFCs consist of a microbe-enriched anode where organic matter is oxidized, and a circuit through which electrons are conducted to typically, an air-fed cathode consisting of a porous carbon structure and an oxygen reduction catalyst, where oxygen is reduced.² Power production from MFCs is often limited by the overpotential of the oxygen reduction reaction (ORR) at the cathode, and the ORR is negatively impacted by the conditions of neutral pH and ambient temperature inherent to MFCs. Depending on the catalyst selected, the ORR proceeds through either a $4e^-$ pathway producing water or hydroxide³ or a $2e^-$ pathway producing hydrogen peroxides as an intermediate.⁴

To limit the large cathode overpotentials, platinum is often used as a catalyst for oxygen reduction, but it is an expensive material and a limited resource. Cathode materials can account for 47–75% of the MFC capital costs,⁵ and therefore it is important to choose less expensive materials as the cathode catalyst. Several catalysts have been considered for use in MFCs, including other metal compounds such as cobalt and

iron tetramethoxyphenylporphyrin (TMPP) or phthalocyanine (Pc)^{6,7} and manganese oxides.^{8,9} Recently, promising results have been obtained using activated carbon (AC) powder based air-cathodes.^{10–13} ACs are especially interesting as they can be made from many different renewable waste materials such as coconut shells, wood chips, and sawdust, making them an inexpensive and renewable resource.

AC powder based cathodes have produced power densities in MFCs similar to or slightly higher than those made with a platinum catalyst. An MFC with an AC cathode made using a proprietary process, which contained a polytetrafluoroethylene (PTFE) binder and a nickel current collector, produced 1220 mW m^{-2} , compared to 1060 mW m^{-2} using a cathode with a Pt catalyst ($0.5 \text{ mg-Pt cm}^{-2}$) and a Nafion binder.¹⁰ An MFC incorporating a similar AC cathode structure that had a polydimethylsiloxane (PDMS) coated cloth diffusion layer reached $1255\text{--}1310 \text{ mW m}^{-2}$ compared to 1295 mW m^{-2} with a standard Pt/C cathode ($0.5 \text{ mg-Pt cm}^{-2}$).¹¹ Using a rolling process to produce a cathode that consisted of an AC/PTFE layer supported by a stainless steel mesh current collector

Received: April 19, 2013

Revised: May 20, 2013

Accepted: May 21, 2013

Published: May 21, 2013

produced 1086 mW m⁻² in an MFC with a high surface area (1701 m² g⁻¹) AC and 1355 mW m⁻² with a lower surface area (576 m² g⁻¹) AC powder. Power production using a standard Pt/C cathode was not reported.¹³ The higher power production by the lower surface area AC cathode was attributed to a more uniform distribution of microporosity. However, only two ACs were compared, and there was no analysis of AC surface chemistry, which could have affected the ORR.

The catalytic activity of ACs and other materials can be evaluated independently of mass transfer limitations using a rotating disk electrode (RDE) and Koutecky–Levich modeling. Because the method requires only a small sample of material and is a relatively quick comparative analysis that allows the researcher to select promising samples for further testing, RDE is a common tool used to evaluate catalysts before testing them as fuel cell cathode catalysts.¹⁴ The evaluation of the material is based on kinetic rates and reaction pathways under non-mass transfer limited conditions. RDE analyses have been used to study the ORR catalysis of many materials, including AC powders¹³ and other materials such as carbon supported magnesium oxide nanoparticles,^{8,9} and FeTMPP and FePc,⁷ where the RDE results were well correlated with MFC performance.

The ORR mechanism at the AC catalyst is not well understood, especially in the neutral pH and phosphate or carbonate buffered solutions used in many MFC studies. Both physical and chemical characteristics of the AC catalyst are important to its performance. The AC surface can contain many different chemical functional groups, and specific surface areas and pore size distributions vary between different materials. The most common heteroatom found in AC functional groups is oxygen, which is present in diverse chemical groups, including acids, such as carboxyl, lactones, and phenol, and weakly basic functionalities, such as ketones, etheric rings, and chromenes.^{15,16} So far, the most extended methodology for testing both functionalities in carbon for use in water phase applications is potentiometric titration (PT).^{4,17–22} This method generates accurate results within a pH range of 3 to 11, due to the buffering power of the water interfering with the quantification of acids stronger than pK_a 3 and bases stronger than 11. To complement PT, XPS is often used to detect groups with a pK_a >10.¹⁸ The use of these methods provides information on the nature and quantity of the functional groups found on the surface of the ACs and insight into their possible role in catalysis.

In order to better understand the factors that affect the performance of AC cathodes in MFCs, nine different ACs made from four different precursor materials were examined as catalysts for oxygen reduction in terms of kinetics and selectivity (based on number of electrons transferred) using RDE tests in neutrally buffered solutions. The catalytic rates obtained under these conditions relevant to MFC operation were then compared in terms of chemical and physical properties that included relative abundance of acidic oxygen functional groups, specific surface area, and pore volume distribution. The results of these kinetic and material property analyses were compared to the power production obtained using different ACs in the cathodes of MFCs.

MATERIALS AND METHODS

Catalyst Materials. Nine different samples were chosen to represent a range of physical and chemical characteristics found in commercially available AC powders. The ACs used were the

following: peat based carbons, Norit SX1 (P1), SXPlus (P2), and SXUltra (P3) (Norit, USA); coconut shell based carbons, YP50 (C1) (Kuraray Chemical, Japan), USP8325C (C2) (Carbon Resources, USA), ACP1250C (C3) (Charcoal House, USA); a hardwood carbon, Nuchar SA-1500 (W1) (MeadWestvaco, USA); a phenolic resin based carbon, RP20 (R1) (Kuraray Chemical, Japan); and a bituminous coal carbon, CR325B (B1) (Carbon Resources, USA). The performance of these carbons in terms of ORR was compared with those of carbon black XC-72 (CB) and Pt (10%) in carbon black XC-72 (PtC) (Fuel Cell Store, USA).

Physical and Chemical Analyses. Detailed incremental surface area and pore volume distributions were determined for each AC from argon adsorption isotherms (at 87.3 K) determined from progressively increasing relative pressures of 10⁻⁶ to 0.993 atm atm⁻¹ (ASAP 2010 Micromeritics Instrument Corp., GA) as described previously.²³ Pore size distributions were calculated from the isotherms using Density Functional Theory (DFT) modeling software (Micromeritics Instrument Corp., GA).²³ Three pore size classifications were used based on the International Union of Pure and Applied Chemistry (IUPAC) definitions, of micropores <2 nm, mesopores between 2–50 nm, and macropores >50 nm.²⁴

The elements present on the surface of the AC powder samples were identified by X-ray photoelectron spectroscopy (XPS) (Axis Ultra XPS, Kratos Analytical, UK, monochrome AlK α source, 1486.6 eV). CASA XPS software was used for the elemental and peak fitting analysis of O1s (531–536 eV) and C1s (285–289 eV) signals.¹⁸

Potentiometric titrations were performed using a DL53 automatic titrator (Mettler Toledo, USA) in the pH range of 3–11. Volumetric standard NaOH (0.1 M) was used as the titrant and NaCl (0.01 M) as the electrolyte. Before titration, 0.2 g of AC was equilibrated with 100 mL of electrolyte at ~pH 3 using HCl (0.1 M) and degassed with N₂ for 1 h. The experimental data were transformed into proton binding curves (Q, mmol g⁻¹), by subtracting the sample titration data to blank titrations.²¹ The proton binding curves were deconvoluted using the SAIEUS numerical procedure to obtain the distribution of acidity constants.^{17,25,26} This analysis produced separate peaks that denoted different types of functional groups, with the area under the peak corresponding to the quantity of functional groups detected (mmol g⁻¹) based on binding/release of protons during titration.

RDE Analysis. Catalyst ink was prepared by adding 30 mg of the powdered sample (except Pt/C which was 6 mg to represent the same loading comparison used in the cathodes) to 3 mL of dimethylformamide (DMF) and homogenized with a sonifier (S-450A, Branson, USA) fitted with a 1/8 in. micro tip, pulsed at 50% for 15 min, in an ice bath. Nafion (5 wt % solution, 270 μ L) was added, and the solution was mixed for an additional 15 min. The ink solution (10 μ L) was drop coated onto a 5 mm diameter glassy carbon disk (Pine Instruments, USA) and allowed to dry overnight. The disk was prepared before coating by polishing with 5.0 and 0.05 μ m alumina paste (Buehler, IL) and cleaned in an ultrasonic bath for 30 min.

All RDE experiments were run first in nitrogen sparged solution, before switching to an air sparged 100 mM phosphate buffer solution (PBS; 9.13 g L⁻¹ Na₂HPO₄, 4.90 g L⁻¹ NaH₂PO₄·H₂O, 0.31 g L⁻¹ NH₄Cl, and 0.13 g L⁻¹ KCl; pH 7). Solutions were sparged for 30 min before linear sweep voltammetry (LSV) was run, and then the gas was streamed into the headspace for the duration of the experiment. In order

to clean the electrode surface of possible contaminants or excess oxygen trapped in the pores of the carbon, the disk potential was cycled between 0.4 and -1.0 V at 100 mV s^{-1} until the current response was the same from cycle to cycle. Then, the potential of the disk electrode was scanned from 0.4 to -1.0 V at 10 mV s^{-1} at rotation rates of 100 to 2100 rpm. The current obtained under nitrogen sparging was subtracted from that obtained under air sparging to obtain the faradaic current due only to oxygen reduction.¹⁴ Catalyst activity was evaluated by the onset potential (E_{onset}) and limiting current (i_{lim}). Kinetic current (i_k) and average number of electrons transferred (n) in the ORR were obtained from the Koutecky–Levich (K–L) analysis⁹ using

$$\frac{1}{i} = \frac{1}{i_k} + \frac{1}{0.62nFAD_{\text{O}_2}^{2/3}\nu^{-1/6}C_{\text{O}_2}\omega^{1/2}} \quad (1)$$

where i is the measured current, i_k is the kinetic current, n is the average number of electrons transferred in the reaction, F is Faraday's constant, A is the projected surface area of the disk electrode, D_{O_2} is the diffusion coefficient of oxygen, ν is the kinematic viscosity, C_{O_2} is the concentration of oxygen in solution, and ω is the rotation rate of the electrode.⁹

MFC Experiments. AC cathodes (31 mg cm^{-2} loading, projected surface area of 7 cm^2) were constructed as previously described,¹¹ except that two PDMS diffusion layers were applied to the air side of the stainless steel mesh current collector (50×50 mesh, type 304, McMaster–Carr, OH) prior to application of the carbons.²⁷ AC powder was mixed with 10 wt % PTFE binder (in a 60% emulsion) and spread evenly onto the solution side and pressed at 4.54 t-force for 20 min (Carver press, Model 4386, Carver Inc., IN).¹¹ Cathodes were made with carbon black (XC-72) following the same technique. Platinum-catalyzed air cathodes (projected surface area of 7 cm^2) were constructed from carbon cloth (30 wt % wet proofing, Fuel Cell Earth LLC) with four PTFE diffusion layers, and a catalyst loading of $0.5 \text{ mg-Pt cm}^{-2}$ (on carbon black XC-72).²⁸

Cube-shaped MFCs were constructed as previously described.²⁹ The anode chamber was a 28 mL cylindrical chamber (7 cm^2 cross section) bored into a Lexan block. The anodes were carbon fiber brushes with a titanium wire core (2.5 cm diameter, 2.5 cm length, and 0.22 m^2 surface area) which was heat treated at 450°C ³⁰ and then placed horizontally in the center of the cylinder. The electrode spacing was 2.5 cm (center of the anode to the face of the cathode). The MFCs were inoculated using effluent from an MFC operated under conditions similar to those used here. The MFC medium was 100 mM PBS amended with vitamins and minerals³¹ and 1 g L^{-1} sodium acetate. Anodes were inoculated and acclimated under the same conditions in MFCs containing standard Pt/C carbon cloth cathodes and then tested with the different cathodes. A 1000Ω resistor was used during acclimation, and then the resistance was changed to lower resistance (100Ω) for several cycles before running polarization tests to avoid power overshoot.³² All MFCs were operated at 30°C in a constant temperature controlled room. Once the MFC produced a steady voltage for 3 cycles, the Pt/C cathodes were removed and replaced with the AC cathodes, CB cathodes, or new Pt/C cathodes. All MFC tests were conducted in duplicate.

The voltage across the resistor was recorded every 30 min using a multimeter (model 2700 Keithley Instruments, Cleveland, OH) with a computerized data acquisition system.

Polarization curves were obtained by applying a different external resistance to the circuit for a complete batch cycle (multiple cycle method), and the average sustainable voltage was recorded for each resistance. Current density was calculated from $I = U/R$, where I is the current, U is the measured cell voltage, and R is the external resistance, and normalized to the projected cathode surface area. Power densities were calculated using $P = IU$ and normalized by the projected cathode surface area.³³

RESULTS AND DISCUSSION

MFC Performance. Based on polarization results, MFCs using cathodes made from different AC powders had quite different maximum power densities (Figure 1A). These ranged

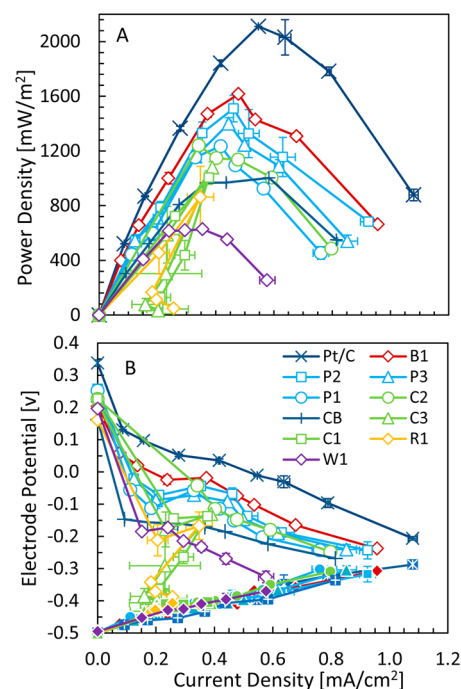


Figure 1. A) Power density production and B) electrode potentials from polarization of MFCs using AC cathodes compared to Pt/C (100 mM phosphate buffer; open symbols represent cathode potentials, closed symbols are anode potentials).

from $1620 \pm 10 \text{ mW m}^{-2}$ ($0.48 \pm 0.00 \text{ mA cm}^{-2}$) using a bituminous coal (B1) to $630 \pm 10 \text{ mW m}^{-2}$ ($0.36 \pm 0.00 \text{ mA cm}^{-2}$) for the hardwood (W1). One of the peat-based cathodes (P2) had a power density of $1610 \pm 100 \text{ mW m}^{-2}$ that was similar to that obtained with cathodes using AC derived from bituminous coal (B1). The MFCs using a standard Pt/C cathode produced a maximum power density of $2110 \pm 0 \text{ mW m}^{-2}$ ($0.55 \pm 0.00 \text{ mA cm}^{-2}$). The lower maximum power densities produced by the AC cathodes were due to decreased cathode potentials (increased cathode overpotentials), as the anodes in all of the MFCs maintained similar working potentials (Figure 1B). The best performing MFCs had cathodes with the lowest overpotentials, as seen with the bituminous sample (B1) operating potential at $-0.07 \pm 0.00 \text{ V}$ (vs Ag/AgCl) at peak power, while the hardwood AC (W1) which had the lowest power operated at $-0.23 \pm 0.01 \text{ V}$ (a 230% decrease in potential). The standard Pt/C cathode potential was $-0.01 \pm 0.00 \text{ V}$.

Catalyst Activity and Selectivity. Catalyst performance evaluated using LSV and RDE produced trends in performance with the different AC precursor materials that generally were similar to those obtained with the MFCs (Figure 2A, Figure

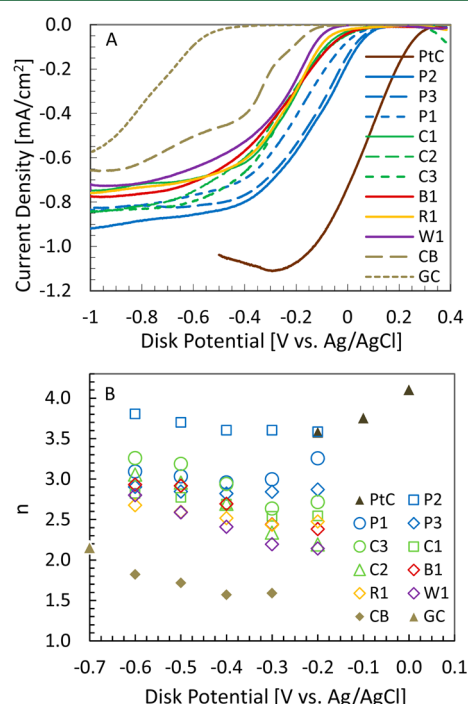


Figure 2. A) LSV current response of the AC catalyst at the disk electrode compared to Pt/C and carbon black (100 mM phosphate buffer, 2100 rpm). B) Average number of electrons transferred (estimated by Koutecky–Levich RDE analysis) during oxygen reduction.

S1). However, the peat-based AC (P2) had the greatest oxygen reduction activity ($E_{\text{onset}} = 0.17$ V and $i_{\text{lim}} = 0.87$ mA cm⁻² at 2100 rpm), and the bituminous coal (B1) sample had only average performance ($E_{\text{onset}} = 0.09$ V and $i_{\text{lim}} = 0.78$ mA cm⁻²), compared to MFC tests where the B1 sample produced a higher peak power density than P2. The hardwood (W1) AC activity in terms of oxygen reduction again had the worst performance ($E_{\text{onset}} = -0.01$ V and $i_{\text{lim}} = 0.73$ mA cm⁻²), but all AC materials had superior performance to carbon black ($E_{\text{onset}} = -0.06$ V and $i_{\text{lim}} = 0.66$ mA cm⁻²) or the plain glassy carbon disk ($E_{\text{onset}} = -0.40$ V and $i_{\text{lim}} = 0.60$ mA cm⁻²). The AC materials also had less catalytic activity than the Pt/C catalyst ($E_{\text{onset}} = 0.36$ V and $i_{\text{lim}} = 1.11$ mA cm⁻²). Catalyst performance was evaluated in RDE tests where diffusion limitations are minimized, compared to conditions in MFC tests where diffusion limitations and concentration gradients likely exist. The difference in performance of the B1 sample (from one of the worst catalysts in RDE tests to the most power production in MFC tests) is therefore likely due to hindered mass transport of reactants and products to and from the active sites limiting the performance of the more porous catalysts. Also, the large amount of AC used in the MFC cathodes, compared to the thin layer used in RDE tests, could have enhanced any diffusion and electrical conductivity limitations.

The performance of the catalysts was examined using the K–L analysis to focus on kinetic current (i_k) and the average number of electrons transferred for oxygen reduction with minimal diffusion limitations (Figure S2). ACs with larger

limiting currents and more positive onset potentials also had higher kinetic current production, where the peat-based (P2) current ($i_k = 1.1$ mA cm⁻² at -0.2 V) was greater than the bituminous coal (B1) ($i_k = 0.5$ mA cm⁻²) and the hardwood (W1) ($i_k = 0.4$ mA cm⁻²) AC catalysts. The selectivity of the catalyst, estimated by the number of electrons transferred in the ORR, of the peat-based (P2) activated carbon catalyst at -0.2 V (Figure 2B) was near four electrons ($n = 3.6$), indicating a mixed reaction that tended toward H₂O/OH⁻ formation either through a direct 4e⁻ reduction or through a series of reductions where the peroxide product was further reduced at the catalyst. The bituminous (B1) ($n = 2.4$) and hardwood (W1) ($n = 2.1$) based samples were closer to a 2e⁻ reduction, where the reduction product was mostly through peroxide formation without further catalytic reduction.⁴ All of the AC powders had increased selectivity compared to carbon black which only reached $n = 2.1$ when the applied potential reached -0.7 V. The electron transfer numbers obtained by other researchers for activated carbons were in the range of $n = 2.6$ – 3.0 at -0.6 V, with $n = 2.1$ at -1.0 V for carbon black.¹³

Effect of Oxygen Functional Groups on ORR Catalysis.

The prevalence and variety of functional groups on the surface of the AC samples, determined by potentiometric titration analysis, influenced their catalytic activity for oxygen reduction. ACs made from the same or similar precursor materials had functional groups with similar pK_a values (Figure 3, Figure S3).

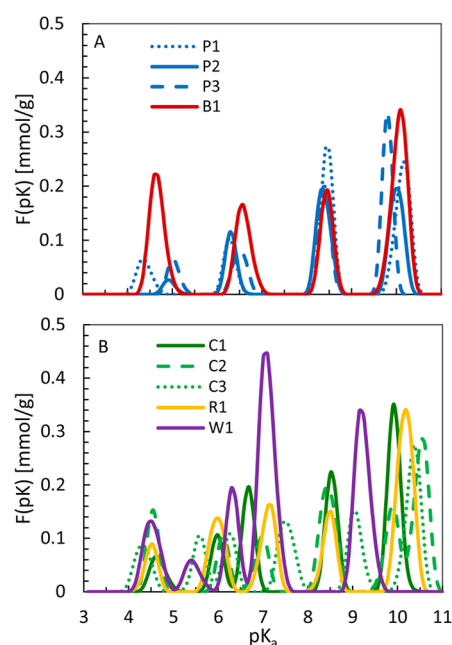


Figure 3. Acidic/oxygen functional groups determined by potentiometric titration. A) Bituminous and peat based activated carbon samples have similar functional groups. B) Other activated carbons have a larger variety of acidic groups.

The two best performing AC samples (P2 and B1) had very similar acidic functional groups present, with peak pK_a values around 4.5, 6.5 (carboxyl-like), 8.5 (lactone-like), and 10 (phenolic-like) (Figure 3A). The quantity (mmol g⁻¹) of acidic functional groups present on the surface of the AC samples, estimated by the area under the curve at each pK_a, varied for the different carbons. There was a greater quantity of strong acid groups (pK_a < 8, typically attributed to carboxyl groups) for the bituminous coal sample (B1, 0.17 mmol g⁻¹) than the three

peat based samples (P1, 0.06 mmol g⁻¹; P2, 0.05 mmol g⁻¹; P3, 0.06 mmol g⁻¹). The ACs made from the other precursor materials showed a larger variety of acidic functional groups (Figure 3B), with the hardwood sample (W1, 0.36 mmol g⁻¹) having the largest quantity of strong acid functional groups. This suggests that the AC surface chemistry, based on the quantity of strong acid groups, had a strong influence on the activity of the AC catalyst for ORR (Figure 4). An increase in

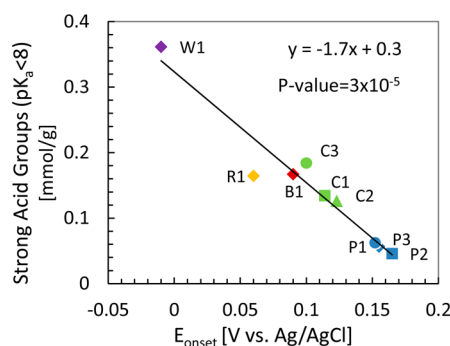


Figure 4. The onset potential of the oxygen reduction reaction is inversely related to the amount of strong acid functional groups present on the activated carbons tested.

strong acid functional groups led to a significant decrease in the onset potential of oxygen reduction ($p = 0.00003$). However, the presence of strong acid functional groups did not correlate as well with the power densities produced when these carbons were used in the cathodes of the MFCs (Figure S4).

Effect of Microporosity on Power Production. The ACs had cumulative surface areas ranging from 550 m² g⁻¹ (B1) to 1440 m² g⁻¹ (R1) and cumulative pore volumes (for pore widths <50 nm) between 0.3 mL g⁻¹ (B1) and 1.1 mL g⁻¹ (W1) (Figure 5, Figure S5). A majority of the surface area was attributed to micropores (Figure 5A). Previous research had shown that the electron transfer number n increased with the area of micropores in carbon powders; however, this trend was not observed here.¹³ With the exception of the hardwood AC (W1), there was a strong inverse relationship between the surface area of the AC powder and the maximum power density achieved in the MFCs. The bituminous sample (B1), which had the least surface area, produced the highest power density in MFC tests, and the phenolic resin sample (R1), which had the most surface area, produced one of the lowest power densities. A similar trend was observed with micropore volume (Figure 5B), where the power density increased inversely with the micropore volume of the carbon. Possibly, the micropores hindered diffusion of the reactants to the catalytic functional sites on the activated carbon as well as the diffusion of the reduction product from the pores, thereby negatively impacting the favorability of the reaction. The observed negative effect of increased microporosity of the AC powders on power production can explain the higher power production of the MFC using the bituminous based cathode (B1) despite the average catalytic performance of the bituminous based AC in the RDE analysis. In the case of the hardwood (W1) based cathode, the poor intrinsic catalytic performance of the hardwood based AC powder (based on RDE tests) likely outweighed the influence of porosity. Most likely there is a combination of factors including porosity, surface chemistry, and conductivity of the AC powders that influence the performance in MFC cathodes.

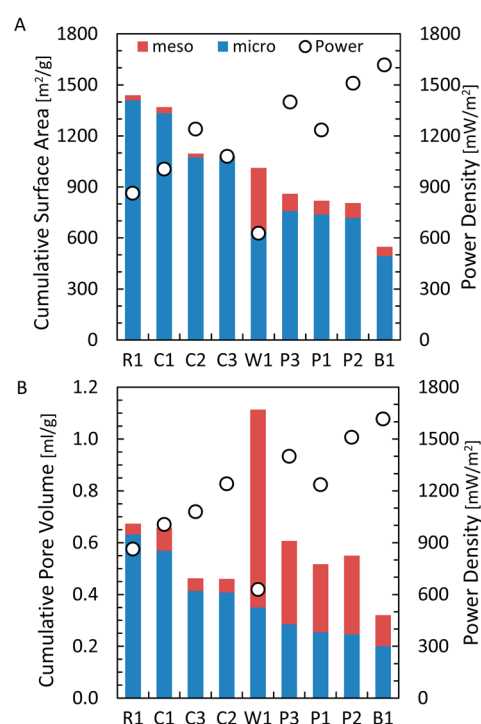


Figure 5. Maximum power density (per m² projected cathode surface) of the MFCs using the activated carbon cathodes is inversely related to the A) surface area (without W1 $p = 0.0006$) and B) micropore volume (without W1 $p = 0.0011$) of the powdered carbons with the exception of sample W1.

Functional Group Analysis Using XPS. The quantity of acidic functional groups measured by potentiometric titration is commonly attributed to oxygen containing groups.¹⁷ Although the onset potential was inversely correlated to the quantity of strong acid/oxygen containing functional groups detected, neither the onset potential nor the power density obtained were correlated with the total atomic percent of oxygen present on the AC surface as determined by XPS (Figure 6A). For instance, the bituminous based AC (B1) had the most oxygen atoms present (9.4%) but only a moderate abundance of strong acid functional groups and average ORR catalytic activity. The chemical state of the oxygen present varied between the samples (Figure 6B), where the bituminous based (B1) sample had a larger amount of oxygen present in the adsorbed O₂/H₂O region (BE = 536–536.6 eV).¹⁸ This suggests that not all oxygen functional groups (e.g., quinones) are detrimental to oxygen reduction catalysis, in agreement with AC ORR catalysis studies using acidic or alkaline media.³⁴ Trace amounts of nitrogen were found in the peat and bituminous samples, with no detectable nitrogen in the remaining samples.

Implications of AC Properties for MFC Performance.

Both the surface chemistry and the pore structure of the AC catalyst affected performance of the catalyst in the cathode of an MFC. AC catalysts selected for neutral buffered environments, like those in MFCs, should have less acidic surface functional groups, which can hinder the ORR activity. Also, the low surface pH of some ACs may cause corrosion at the interface of the AC and the stainless steel mesh, which may increase the ohmic resistance of the cathode. The effect of basic (rather than acidic) functional groups on ORR catalysis should be further investigated. ACs used in MFC cathodes should not be chosen solely because they have the largest surface area, but

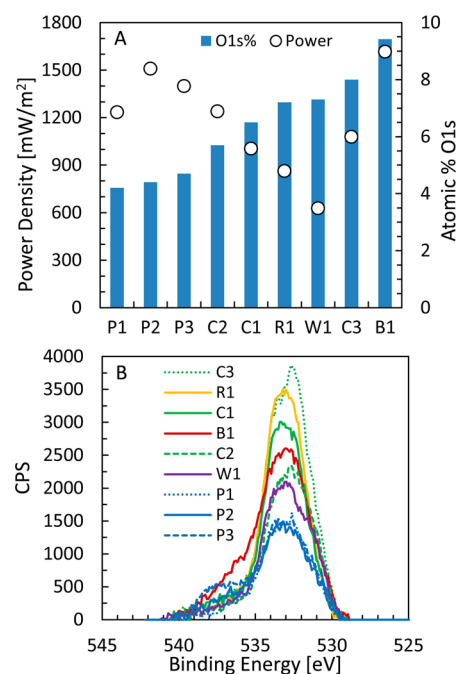


Figure 6. A) Maximum power density of the MFCs with activated carbon cathodes are not directly related to the oxygen content of the activated carbon powders determined by XPS. B) Chemical state of the oxygen detected by XPS varies for activated carbon powders tested (e.g., increased signal in the adsorbed O_2/H_2O region for sample B1).

instead ACs should be selected that have a moderate amount of micropore volume and surface area to avoid the negative impact of diffusion limitations to the active catalyst sites. The conductivity of different ACs may also influence on the performance of the AC cathodes. Binders, AC loading, and manufacturing methods can affect the diffusion characteristics of the cathodes and their performance relative to standard Pt/C cathodes,^{11,13} and therefore this aspect of cathode construction should also be taken into consideration when constructing MFC cathodes. Longevity of AC catalysts in MFC cathodes is also an issue for MFC applications,³⁵ and therefore changes in surface chemistry and rates of mass transfer to catalytic sites should also be considered in future studies.

■ ASSOCIATED CONTENT

● Supporting Information

Additional figures as referenced in text, including RDE analysis, proton binding isotherms, and pore volume distribution. This material is available free of charge via the Internet at <http://pubs.acs.org>.

■ AUTHOR INFORMATION

Corresponding Author

*Phone: +1-814-863-7908. Fax: +1-814-863-7304. E-mail: blogan@psu.edu.

Notes

The authors declare no competing financial interest.

■ ACKNOWLEDGMENTS

The authors thank Vince Bojan for assistance with XPS analysis. The authors acknowledge support from the King Abdullah University of Science and Technology (KAUST) by Award

KUS-I1-003-13 and the National Science Foundation Graduate Research Fellowship Program (NSF-GRFP).

■ REFERENCES

- (1) Logan, B.; Rabaey, K. Conversion of wastes into bioelectricity and chemicals by using microbial electrochemical technologies. *Science* **2012**, *337*, 686–690.
- (2) Logan, B. E. *Microbial Fuel Cells*; John Wiley & Sons: Hoboken, NJ, 2008.
- (3) Popat, S.; Dongwon, K.; Rittmann, B. E.; Torres, C. I. Importance of OH^- transport from cathodes in microbial fuel cells. *ChemSusChem* **2012**, *5*, 1071–1079.
- (4) Zhong, R.-S.; Qin, Y.-H.; Niu, D.-F.; Tian, J.-W.; Zhang, X.-S.; Zhou, X.-G.; Sun, S.-G.; Yuan, W.-K. Effect of carbon nanofiber surface functional groups on oxygen reduction in alkaline solution. *J. Power Sources* **2013**, *225*, 192–199.
- (5) Rozendal, R. A.; Hamelers, H. V. M.; Rabaey, K.; Keller, J.; Buisman, C. J. N. Towards practical implementation of bioelectrochemical wastewater treatment. *Trends Biotechnol.* **2008**, *26* (8), 450–459.
- (6) Yu, E. H.; Cheng, S.; Scott, K.; Logan, B. Microbial fuel cell performance with non-Pt cathode catalysts. *J. Power Sources* **2007**, *171*, 275–281.
- (7) Birry, L.; Mehta, P.; Jaouen, F.; Dodelet, J. P.; Guio, S. R.; Tartakovsky, B. Application of iron-based cathode catalysts in a microbial fuel cell. *Electrochim. Acta* **2011**, *56*, 1505–1511.
- (8) Roche, I.; Scott, K. Carbon-supported manganese oxide nanoparticles as electrocatalysts for oxygen reduction reaction (orr) in neutral solution. *J. Appl. Electrochem.* **2009**, *39*, 197–204.
- (9) Chen, Y.; Lv, Z.; Xu, J.; Peng, D.; Liu, Y.; Chen, J.; Sun, X.; Feng, C.; Wei, C. Stainless steel mesh coated with MnO_2 /carbon nanotube and polymethylphenyl siloxane as low-cost and high-performance microbial fuel cell cathode materials. *J. Power Sources* **2012**, *201*, 136–141.
- (10) Zhang, F.; Cheng, S.; Pant, D.; Van Bogaert, G.; Logan, B. Power generation using an activated carbon and metal mesh cathode in a microbial fuel cell. *Electrochem. Commun.* **2009**, *11* (11), 2177–2179.
- (11) Wei, B.; Tokash, J. C.; Chen, G.; Hickner, M. A.; Logan, B. E. Development and evaluation of carbon and binder loading in low-cost activated carbon cathodes for air-cathode microbial fuel cells. *RSC Adv.* **2012**, *2*, 12751–12758.
- (12) Dong, H.; Yu, H.; Wang, X.; Zhou, Q.; Feng, J. A novel structure of scalable air-cathode without Nafion and Pt by rolling activated carbon and PTFE as catalyst layer in microbial fuel cells. *Water Res.* **2012**, *46*, 5777–5787.
- (13) Dong, H.; Yu, H.; Wang, X. Catalysis kinetics and porous analysis of rolling activated carbon-PTFE air-cathode in microbial fuel cells. *Environ. Sci. Technol.* **2012**, *46*, 13009–13015.
- (14) Gojkovic, S. L.; Gupta, S.; Savinell, R. F. Heat-treated iron(III) tetramethoxyphenyl porphyrin supported on high-area carbon as an electrocatalyst for oxygen reduction - I. Characterization of the electrocatalyst. *J. Electrochem. Soc.* **1998**, *145*, 3493–3499.
- (15) Radovic, L. R.; Moreno-Casilla, C.; Rivera-Utrilla, J. Carbon materials as adsorbents in aqueous solutions. *Chem. Phys. Carbon* **2001**, *27*.
- (16) Fuente, E.; Menendez, J. A.; Suarez, D.; Montes-Moran, M. A. Basic surface oxides on carbon materials: a global view. *Langmuir* **2003**, *19*, 3505–3511.
- (17) Bandoz, T. J.; Jagiello, J.; Contescu, C. Characterization of the surfaces of activated carbons in terms of their acidity constant distributions. *Carbon* **1993**, *31* (7), 1193–1202.
- (18) Seredych, M.; Bandoz, T. J. Investigation of the enhancing effects of sulfur and/or oxygen functional groups of nanoporous carbons on adsorption of dibenzothiophenes. *Carbon* **2011**, *49*, 1216–1224.
- (19) Szymanski, G. S.; Zbigniew, K.; Biniak, S.; Swiatkowski, A. The effect of the gradual thermal decomposition of surface oxygen species

on the chemical and catalytic properties of oxidized activated carbon. *Carbon* **2002**, *40*, 2627–2639.

(20) Neffe, S. Evaluation of the pH-metric method for the determination of acidic groups on the surface of oxidized carbons. *Carbon* **1987**, *25*, 441–443.

(21) Jagiello, J.; Bandosz, T. J.; Schwarz, J. A. Carbon surface characterization in terms of its acidity constant distribution. *Carbon* **1994**, *32*, 1026–1028.

(22) Puziy, A. M.; Poddubnaya, O. I.; Ritter, J. A.; Ebner, A. D.; Holland, C. E. Elucidation of the ion binding mechanism in heterogeneous carbon-composite adsorbents. *Carbon* **2001**, *39*, 2313–2324.

(23) Moore, B. C.; Cannon, F. S.; Westrick, J. A.; Metz, D. H.; Shrive, C. A.; DeMarco, J.; Hartman, D. J. Changes in GAC pore structure during full-scale water treatment at Cincinnati: a comparison between virgin and thermally reactivated GAC. *Carbon* **2001**, *39*, 789–807.

(24) Rouquerol, J.; Avnir, D.; Fairbridge, C. W.; Everett, D. H.; Haynes, J. M.; Pernicone, N.; Ramsay, J. D. F.; Swing, K. S. W.; Unger, K. K. Recommendations for the characterization of porous solids. *Pure Appl. Chem.* **1994**, *66* (8), 1739–1758.

(25) Jagiello, J. Stable numerical solution of the adsorption integral equation using splines. *Langmuir* **1994**, *10* (8), 2778–2785.

(26) Bandosz, T. J.; Jagiello, J.; Krzyzankowski, A.; Schwarz, J. A. Effect of surface chemistry on sorption of water and methanol on activated carbons. *Langmuir* **1996**, *12*, 6480–6486.

(27) Zhang, X.; Cheng, S.; Huang, X.; Logan, B. E. Improved performance of single-chamber microbial fuel cells through control of membrane deformation. *Biosens. Bioelectron.* **2010**, *25*, 1825–1828.

(28) Cheng, S.; Liu, H.; Logan, B. E. Increased performance of single-chamber microbial fuel cells using an improved cathode structure. *Electrochem. Commun.* **2006**, *8*, 489–494.

(29) Liu, H.; Ramnarayanan, R.; Logan, B. E. Production of electricity during wastewater treatment using a single chamber microbial fuel cell. *Environ. Sci. Technol.* **2004**, *38* (7), 2281–2285.

(30) Feng, Y.; Yang, Q.; Wang, X.; Logan, B. E. Treatment of carbon fiber brush anodes for improving power generation in air-cathode microbial fuel cells. *J. Power Sources* **2010**, *195*, 1841–1844.

(31) Bretschger, O.; Obratsova, A.; Sturm, C. A.; Chang, I. S.; Gorby, Y. A.; Reed, S. B.; Culley, D. E.; Reardon, C. L.; Barua, S.; Romine, M. F.; Zhou, J.; Beliaev, A. S.; Bouhenni, R.; Saffarini, D.; Mansfeld, F.; Kim, B.-H.; Fredrickson, J. K.; Nealson, K. H. Current production and metal oxide reduction by *Shewanella oneidensis* MR-1 wild type and mutants. *Appl. Environ. Microbiol.* **2007**, *73* (21), 7003–7012.

(32) Hong, Y.; Call, D.; Werner, C. M.; Logan, B. E. Adaptation to high current using low external resistances eliminates power overshoot in microbial fuel cells. *Biosens. Bioelectron.* **2011**, *28* (1), 71–76.

(33) Logan, B. E.; Aelterman, P.; Hamelers, B.; Rozendal, R.; Schröder, U.; Keller, J.; Freguiac, S.; Verstraete, W.; Rabaey, K. Microbial fuel cells: methodology and technology. *Environ. Sci. Technol.* **2006**, *40* (17), 5181–5192.

(34) Song, C.; Zhang, J. Electrocatalytic oxygen reduction reaction. In *PEM Fuel Cell Electrocatalysts and Catalyst Layers: Fundamentals and Applications*; Zhang, J., Ed.; Springer: London: 2008; pp 89–134.

(35) Zhang, F.; Pant, D.; Logan, B. E. Long-term performance of activated carbon air cathodes with different diffusion layer porosities in microbial fuel cells. *Biosens. Bioelectron.* **2011**, *30* (1), 49–55.